MÖSSBAUER AND XRD ANALYSIS OF CORROSION PRODUCTS OF CARBONATED ALKALI-ACTIVATED SLAG REINFORCED CONCRETES

ANÁLISIS DE LOS PRODUCTOS DE CORROSIÓN DE ACEROS EMBEBIDOS EN HORMIGÓN DE ESCORIA ACTIVADA ALCALINAMENTE EXPUESTO A CARBONATACIÓN

WILLIAN APERADOR

PhD. Profesor: Universidad Militar Nueva Granada. Bogotá, Colombia, william.aperador@unimilitar.edu.co

JORGE BAUTISTA

MSc. Profesor: Universidad Francisco de Paula Santander, Cúcuta, Colombia, jorgebautista@ufps.edu.co

ENRIQUE VERA

PhD. Profesor: Universidad Pedagógica y Tecnológica de Colombia, Tunja., enrique.vera@uptc.edu.co

Received for review: January 12th, 2011; accepted: May 17rd, 2011; final version: May 30nd, 2011

ABSTRACT: Steel bars embedded in an alkali-activated slag (AAS) concrete have been exposed (after curing for 28 days) to an accelerated carbonation chamber (3 % CO2, 65 % relative humidity (RH), and 25 ºC temperature) and to a laboratory environment (0.03 % CO_2, 65 % RH, and 25 ºC). Ordinary Portland cement (OPC) was also tested for comparative purposes and exposed to identical experimental conditions. Corrosion products generated at the steel/concrete interface were characterized using Mössbauer spectrometry and the X-ray diffraction (XRD) technique. The main compounds were magnetite (Fe3O4), wuestite (FeO), and goethite (a-FeOOH). The morphology of corrosion products was analyzed using the scanning electron microscopy technique (SEM).

KEYWORDS: carbonation, corrosion, magnetite, wuestite, alkali-activated cement, Portland cement, steel reinforcement

RESUMEN: Barras de acero embebidas en el hormigón de escoria activada alcalinamente (AAS) fueron expuestas (después de los 28 días de curado) en una cámara de carbonatación acelerada (3% CO_2, 65% de humedad relativa (HR) y 25 º C de temperatura) y un entorno de laboratorio (0,03% CO2, 65% HR y 25 º C). Cemento Portland (OPC), se probó también con fines comparativos y expuestos a las mismas condiciones experimentales. Los productos de corrosión generados en la interfase acero / concreto se caracterizaron utilizando espectrometría Mössbauer y la técnica de difracción de rayos X (DRX). Los principales componentes fueron la magnetita (Fe_3O_4), wuestite (FeO) y goethita (a-FeOOH). La morfología de los productos de corrosión se analizó mediante la técnica de microscopía electrónica de barrido (SEM).

PALABRAS CLAVE: Carbonatación, corrosión, magnetita, wuestita, cemento activado alcalinamente, cemento portland, acero de refuerzo.

1. INTRODUCTION

Nature and the integrity of the layer of solid hydration products formed in close proximity to embedded steel may have an important role in controlling the passivation and depassivation of the metal.

The very high temperatures (1400–1500 ºC) required for manufacturing ordinary Portland cement (OPC), which make it responsible for 40 % of all energy consumed, account for the extremely high costs of this process. The environmental impact attributed to the manufacturing of OPC is largely due to the energy-intensive processes involved. Indeed, the cement industry is regarded to be responsible for 6-7 % of all greenhouse gases emitted world-wide [1].

In an attempt to overcome these problems, the construction sector is very interested in the development of new cement binder materials as an alternative to OPC [2, 3]. In this respect, the most promising emerging approach is based on new raw materials suitable for

alkaline activation, which originate new binding materials generically known as alkaline cements [4]. Granulated blast-furnace slag (GBFS) has been used for many years as a supplementary cementitious material (SCM) in OPC concrete, either as a mineral admixture or as a component of blended cement [5]. The GBFS experiments a rapid hydration when it is mixed with an appropriate trigger as a sodium silicate solution, and if it is mixed with aggregates it can produce a concrete that presents a high mechanical resistance at early ages. It generates a dense and airtight concrete [6,7].

The GBFSs are the result of the combination of clay acid iron material and the sulphurous ashes of coke (also with acid properties), with lime, and the dolomite limestone used for the melting of magnesia (both basic compounds). The combination of acid oxides (CaO and MgO) and the formation of the slag compounds occur by melting at high temperatures (~1600 ºC), and the cooling of the magmatic fluid from 1400 °C to room temperature [8,9].

The aim of this paper was to study the corrosion products generated on steel rebars embedded in artificially carbonated AAS (3 % by volume of CO_2). The results were compared with steel embedded in OPC. Corrosion products were studied to characterize the steel/concrete interface using Mössbauer spectrometry and the X-ray diffraction (XRD) technique. The morphology of corrosion products was analyzed using the scanning electron microscopy technique (SEM).

2. EXPERIMENTAL SET-UP

Ground granulated blast furnace slag (GBFS) cementitious materials from the Company *Acerias Paz del Rio*, located in Boyaca, Colombia, were used having a chemical composition of 33.7 % SiO_2, 12.8 % Al_2O_3, 45.4 % CaO, 0.5 % TiO_2, and 1.0 % MgO, a specific surface of 398 m^2 kg^{-1} and a specific gravity of 2860 kg m^{-3}. The basicity (CaO + MgO / SiO_2 + Al_2O_3) and quality (CaO + MgO + Al_2O_3 / SiO_2 + TiO_2) indexes were 1.01 and 1.73, respectively. According to the ASTM C 989 - 99 standard, this material was grade 80 slag [10]. The waterglass used as the activating solution consisted in a mix of commercial sodium silicate (31.7 % SiO_2, 12.3 % Na_2O, and 56.0 % water) with a 50 % NaOH solution to obtain an SiO_2 / Na_2O ratio of 2.4. The Na_2O concentration in the waterglass activating solution added to the concretes was 5 % by slag weight.

The aggregate used was a siliceous gravel with a maximum grain size of 19 mm, a specific gravity of 2940 kg m^{-3}, and 1.3 % absorption; and river sand with a maximum grain size of 19 mm, a specific gravity of 2470 kg m^{-3}, and 2.9 % absorption. Commercial Portland cement (OPC), according to the ASTM C 150-02 standard was used for comparative purposes [11]; its specific gravity and specific surface were 2990 kg m^{-3} and 400 kg m^{-3}, respectively. Alkali-activated slag and OPC concretes were prepared having a water/cementitious material ratio of 0.4. It was assumed that the water/cement ratio was equivalent to the (water + activator) / slag ratio.

The AAS and OPC specimens were cured in a climatic chamber for 28 days at 90 % relative humidity (RH) for AAS specimens and at 100 % RH for OPC specimens to prevent leaching of the activating solutions and to assure that the hydration reaction and product formation processes were not affected.

An accelerated carbonation chamber was used, with 3 % CO_2 by volume, 65 % RH, and 25 ºC (specimens AASA and OPCA). Additionally, a second carbonation test was performed by exposition to a laboratory environment condition, having 0.03 % CO_2 by volume, 65 % RH, and 25 ºC (specimens AASL and OPCL).

Structural 1018 steel bars of 6.35 mm diameter were used, according to the ASTM A 706-08 standard [12]. A reinforced concrete cylindrical specimen (76.2 mm diameter and 76.2 mm length) was used to perform experimental tests.

At the end of the experiments, the specimens were broken and the steel/concrete interface was analyzed. An alcoholic dissolution of 1 % phenolphthalein indicator was applied on the fresh fractured surfaces of the specimens to measure carbonation depth with elapsed time. On AAS concrete exposed to the accelerated carbonation phenomenon (3 % CO_2) a pH reduction was observed of values near to 9. The pH value was calculated as the average of 7 results obtained along the radius of the specimens.

Corrosion products were characterized using the Mössbauer spectrometry technique. The spectra analysis was performed using the Mosfit Program and the values of isomer shift are quoted relative to that of a-Fe at 300 K [13].

The solid crystalline phases present in the corrosion products formed on the steel/concrete interfaces were characterized by XRD, using an X'PERT PRO MRD (Panalytical, B.V.) diffractometer with monochromatized Cu Ka radiation at 45 kV and 40 mA, and a Xe proportional detector. Parallel beam optics were used, consisting of a parabolic mirror in the incident beam and a 0.18º parallel plate collimator with a flat graphite monochromator in the diffracted beam. X-ray analysis was recorded from 5 to 65 2q degrees, in the step-scanning mode, with 0.03º (2q) step and 2 s counting time.

Scanning electron microscopy (SEM) and energy dispersive X-ray (EDX) techniques were applied using a JEOL JXA-840 equipped with a LINK AN 10 000 system.

3. RESULTS AND DISCUSSION

In the literature it has been reported that there are zones that might correspond to decalcified precipitates of calcium-silicate-hydrate (C-S-H) gel formed in the course of the carbonation phenomenon between AAS and iron carbonate. Since the Na is very soluble and gradually lost in the matrix of the AAS when concrete is exposed to CO_2, only the Ca of the C-S-H gel can protect the pH in the pore solution [14]. However, the Ca/Si ratio in the C-S-H of the AAS concrete is close to 1, while OPC concrete is 1.7–2.0. Therefore, the AAS concrete has a low capacity for keeping the pH of the pore solution. The C-S-H in the AAS concrete is transformed to calcium and C-S-H is decalcified, which is rich in silicon [15]. Thus, when the AAS concrete is exposed to CO_2, the C-S-H gel reacts by producing calcium carbonate ($CaCO_3$), C-S-H decalcification, and aluminosilicates. As a result of the reaction of the carbonates, the porosity in the matrix may increase; which favors the depositing of carbonates (CO_3^{2-}) and CO_2 in the concrete. Consequently, the reaction front penetrates easily within the concrete. Reported results showed higher carbonation rates for AAS than for OPC [16,17]. The carbonation of AAS concrete occurs directly on the C-S-H gel originating a lower Ca content, silica gel, and alumina phase [18,19].

Figures 1 and 2 show the Mössbauer spectra recorded at 300 K for AAS and OPC concretes exposed to accelerated carbonation and to a laboratory environment. They were obtained assuming a linear correlation between the distribution of hyperfine fields and isomer shift, to describe the asymmetry. Both AAS and OPC concretes showed a similar behavior. The main compounds identified were magnetite (Fe_3O_4), wuestite (FeO), and goethite (a-FeOOH), see Table 1. The spectra were fitted using the following components: two sextets attributed to the espinel phase of magnetite, one sextet attributed to the iron phase, one doublet attributed to the wuestite phase, and one doublet attributed to the goethite phase.

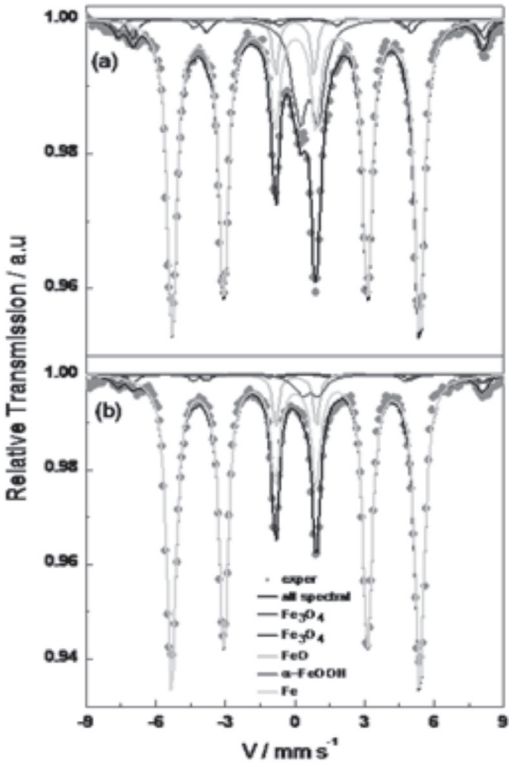

Figure 1. Mössbauer spectra for steel bars embedded in AAS concrete exposed to (a) unpolluted laboratory environment (specimen AASL), and (b) to accelerated carbonation chamber (specimen AASA)

Table 1. Phase percentage obtained from the Mössbauer spectrometry obtained at the end of the experiments. The concretes AASA and OPCA were exposed to an accelerated carbonation chamber, and the concretes AASL and OPCL were exposed to a laboratory environment (*Universidad del Valle*, Cali).

Concrete	Phase Characterized, %			
	Magnetite (Fe_3O_4)	Wuestite (FeO)	Goethite (a-FeOOH)	Iron
AASA	6.4	3.71	13.88	76.01
AASL	3.95	4.11	3.45	88.49
OPCA	5.75	2.31	7.72	84.22
OPCL	6.76	3.31	6.63	83.29

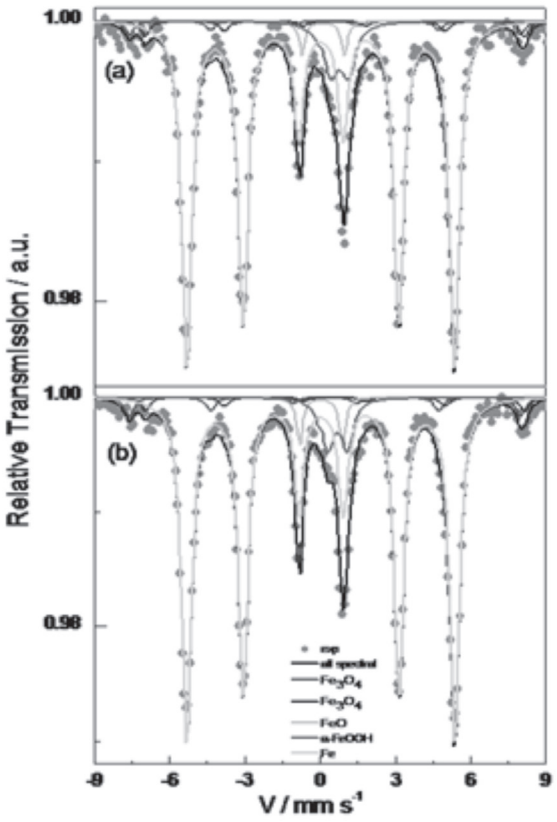

Figure 2. Mössbauer spectra for steel bars embedded in OPC concrte exposed to (a) unpolluted laboratory environment (specimen OPCL), and (b) to accelerated carbonation chamber (specimen OPCA)

Characterization of the corrosion products by XRD analysis allowed the detection of the following crystalline phases: magnetite (Fe_3O_4), file 05-0667 of the International Center for Diffraction Data (ICDD), strong lines at 36.417, 42.295, and 61.341 (º); wuestite (FeO), ICDD file 42-0638, strong lines at 13.329, 26.896, and 35.654 (º); and goethite (a-FeOOH), ICDD file 50-0663, strong lines at 13.088 and 26.284 (º).

Figures 3 and 4 show representative XRD patterns recorded from 5 to 65 2q degrees for steel/concrete specimens cured for 28 days and exposed to accelerated carbonation and laboratory environment for 45 days of experimentation. In Fig. 3, the XRD patterns reveal the reflections (111) and (200) of metallic steel, file 04-0836, at 43.295 and 50.431 (º). In addition to metallic steel peaks, the reflection (111) of magnetite can be observed at 36.417 (º). The presence of wuestite can also be observed on the patterns for 45 days at 16.920 (º).

The analysis was performed by XRD on the surface of steel embedded in AAS and OPC concrete to appreciate the presence of oxides and hydroxides of iron in all samples analyzed in the laboratory environment). Other components that appear in the XRD analysis are attributed to the constituents that concrete and aggregates.

Figure 3 shows that the spectrum of XRD from the surface of the steel sample was embedded in slag activated alkali after being subjected to 45 days accelerated exposure to CO_2..

It is in this circumstance that one can find the following phases present: C: calcite, G: goethite, AN: andradite, MG: magnetite, W: wüstite, L: lepidocrocite, HM: hematite and Q: quartz. Magnetite and W oxides are the most predominant in the steel surface. These iron oxides are present in most of the corrosion processes; MG temperature is generated even before the steel embedded in concrete analyzed is subjected to the process of carbonation or environmental exposure. The hydroxides G, L, and HM are found, where the phase corresponding to G is occurring with greater intensity on the surface studied. In Fig. 3 it can be seen that the peaks in the diffractograms of AASA and AASC overlap each other, showing approximately the same intensity for the phase called calcite.

Figure 4 observed diffractograms obtained for the steel embedded in Portland cement-based concrete. In the OPCL there are some stages with greater intensity than those found with the OPCA, which is due to the formation of the protective layer which is generated from oxides and hydroxides. We found the following phases present: SC (calcium silicate), C, G, AN, MG, W, L, HM, and Q.

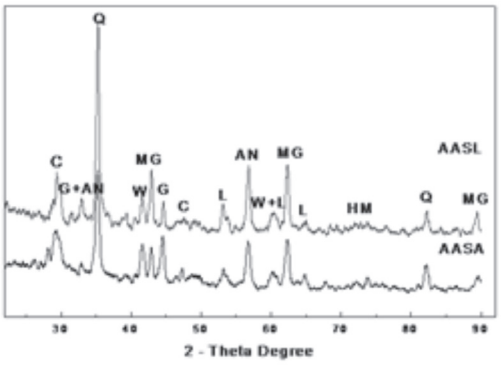

Figure 3. XRD patterns for specimens exposed to the laboratory environment (specimen AASL), and (b) to accelerated carbonation (specimen AASA)

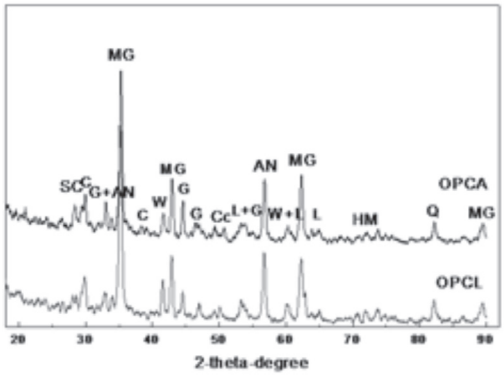

Figure 4. XRD patterns for specimens exposed to the laboratory environment (specimen OPCL), and (b) to accelerated carbonation (specimen OPCA)

4. CONCLUSIONS

The nature and integrity of the layer of solid corrosion products formed in close proximity to embedded steel may have not an important role in controlling the passivation and the depassivation of the steel rebar. Finally, it would also seem appropriate to emphasize that the observations and conclusions cannot be expected to apply generally to Portland and alkali-activated slag concretes.

ACKNOWLEDGEMENTS

W. Aperador expresses his gratitude to the CENM and COLCIENCIAS of Colombia, Project Geoconcret, for the scholarship granted. D. M. Bastidas expresses his gratitude for project BIA2008-05398 from the CICYT, Spain, for financial support.

REFERENCES

[1] Fernández-Jiménez, A.M., Palomo, A., López-Hombrados, C., Engineering properties of alkali-activated fly ash concrete, ACI Materials Journal 103, pp.106-112, 2006.

[2] Moreno, M. Morris, W. Alvarez, M.G., Duff, G.S. Corrosion of reinforcing steel in simulated concrete pore solutions. Effect of carbonation and chloride content, Corros Sci 46, pp. 2681-2699, 2004.

[3] Torres, R. Aperador, W. Vera E. Estudio de la corrosión del acero embebido en concreto aas sometido a cloruros. Dyna, Año 77, Nro. 164, pp. 52-59, 2010

[4] Fernández-Jimenez, A., Puertas, F. Effect of activator mix on the hydration and strength behaviour of alkali-activated slag cements, Adv Cem Res 15, pp. 129-136, 2003.

[5] Song, H.W., Saraswanthy, V. Studies on the corrosion resistance of reinforced steel in concrete with ground granulated blast-furnace slag. An overview, J Hazard Mater 138, pp. 226-233, 2006.

[6] Mejía de Gutiérrez, R., Maldonado, J., Delvasto, S., Puertas, F., Fernández-Jiménez, A. Durability of mortars made with alkali activated slag, 11th Int. Congress on the Chemistry of Cement, ICCC, Durban, South Africa, vol. 1, pp. 1005-1012, 2003,

[7] Rodríguez, E., Bernal, S., Mejía de Gutierrez, R., Puertas, F. Alternative concrete base on alkali-activated slag, Mater Construcc. 58, pp. 53-67, 2008.

[8] Torres R, Aperador W., Vera E., Mejía de Gutierrez., Ortiz C. Estudio de la corrosión del acero embebido en concreto AAS sometido a cloruro, Dyna Año 77, Nro. 164, pp. 5259.

[9] Puertas, F. Cementos de escorias activadas alcalinamente: Situación actual y perspectivas de futuro, Mater Construcc. 45, pp. 53-64, 1995.

[10] ASTM C 989-99 Standard, Standard specification for ground granulated blast-furnace slag for use in concrete and mortars, West Conshohocken, PA, American Society for Testing and Materials, 1999.

[11] ASTM C 150-02 Standard, Specification for Portland cement test, West Conshohocken, PA, American Society for Testing and Materials, 2002.

[12] ASTM A 706-08 Standard, Standard specification for low-alloy steel deformed and plain bars for concrete reinforcement, West Conshohocken, PA, American Society for Testing and Materials, 2008.

[13] Rodríguez, R.R., Pérez-Alcáraz, G.A. Sánchez, H., Greneche, J.M. Milling time effects on the magnetic and structural properties of the $Fe_{70}Si_{30}$ system, Microelectron J 39, pp. 1311-1313. 2008.

[14] Bakhareva, T., Sanjayana, J.G., Cheng, B. Resistance of alkali-activated slag concrete to carbonation, Cement Concrete Res 31 pp. 1277-1283, 2001.

[15] WANG, S.D. SCRIVENER, K. Hydration products of alkali activated slag cement, Cement Concrete Res 25, 561-571, 1995.

[16] Byfors, K., Klingstedt, G., Lehtonen, V., Pyy, H., Romben, L. Durability of concrete made with alkali-activated slag, Proceedings 3rd CANMET/ACI International Conference, Trondheim, Norway, ACI, Detroit, vol. 2, pp. 1429-1466, 1989.

[17] Pu, X.C., Gan, C.C., Wang, S.D., Yang, C.H., Summary reports of research on alkali-activated slag cement and concrete, Chongqing Institute of Architecture and Engineering, Chongqing 1-6, 1988.

[18] Palacios, M., Puertas, F. Effect of carbonation on alkali-activated slag paste, J Am Ceram Soc 89, pp. 3211-3221, 2006.

[19] Schiessl, P. (Editor), New Approach to Durability Design-An example for carbonation inducced corrosion, Comité Euro-International du Béton, CEB Bulletin, No. 238, Lausanne, Switzerland, 1997.